2018

Haloferax volcanii for carotenoid production

Erika Smith
Colby College

Haloferax volcanii for carotenoid production

By Erika Smith

Approved:

_____

(Mentor. Ron Peck, Assistant Professor of Biology)

_____Date

_____

(*Reader. Rebecca Conry, Associate Professor of Chemistry)*

_____Date

VITAE

Erika Smith graduated as a valedictorian from Salem High School, Salem, NH in 2014. While at Colby, Smith majored in chemistry with a concentration in biochemistry. From January 2016 to August 2016, Smith worked for Professor Nicholas Boekelheide, using molecular dynamic simulations to study active site interactions in ribulose-1,5-bisphosphate carboxylase/oxygenase (RubisCO), which is the enzyme catalyzing the first step of the Calvin Cycle. During January of 2017, Smith joined Professor Ronald Peck's lab, where she studied protein interactions and the physiology of halophilic archaea. She was awarded the INBRE Summer Student Fellowship, which permitted her to continue her work in the lab during the summer of 2017. A four-year high school varsity field hockey and lacrosse player and a captain of both during her senior year, Smith also played 3 seasons of field hockey during her time at Colby. In the fall of 2018, Smith will be matriculating in the Biochemistry, Cellular, and Molecular Biology PhD. program at the Johns Hopkins University School of Medicine.

Acknowledgements

I would like to thank Professor Ron Peck for the support and guidance on this project, as well as Professor Rebecca Conry for being a reader to this thesis. Additionally, I would like to thank Serena Graham, Alex Pleşa ‘17, Emily Shaw ‘19, Abby Gregory ‘19, Sammy Scofield ’20, and the rest of the Peck lab for their help. This project was in part funded by the Maine IDeA Network of Biomedical Research Excellence (INBRE) Summer Research Fellowship program as well as by NIH grant P20-RR-016463. This project was made possible with the funding, facilities, and support provided by Colby College Biology and Chemistry departments.

Table of Contents

Abstract

Carotenoids are used as natural colorants and have been shown to have numerous health benefits, making these molecules highly desirable in the aquaculture, pharmaceutical, and nutraceutical markets. There is increasing consumer demand for the natural synthesis of carotenoids, but current methods are limited by the cost and difficulty of extraction from organisms. The halophilic archaeon *Haloferax volcanii* is amenable to extraction and has an endogenous carotenoid biosynthetic pathway that culminates in the accumulation of the carotenoid bacterioruberin; however, *H. volcanii* also synthesizes important precursors that can be converted into more highly-desired carotenoids, such as β-carotene and astaxanthin, in the presence of enzymes that catalyze these reactions. In this work, we show that the carotenoid biosynthetic pathway in *H. volcanii* can be manipulated to increase overall carotenoid production and to synthesize carotenoids of high demand. Insertion of a highly active promoter resulted in significantly increased lycopene and phytoene production, while expression of a nonnative gene encoding the lycopene cyclase enzyme allowed for β-carotene synthesis. These results may inform future work investigating the use of *H. volcanii* for the bioproduction of carotenoids on an industrial scale.

Introduction

Carotenoids are light-absorbing pigments produced naturally by many plants and microorganisms. These isoprenoid compounds are synthesized by linking two C_{20} geranylgeranyl pyrophosphate (GGPP) molecules to produce a C_{40} skeleton from which each carotenoid is derived (Fig. 1). Modifications to this parent structure include cyclization at the ends of the molecule, the addition of oxygen-containing functional groups, and changes in hydrogenation level. These modifications lead to two major classes of carotenoids: (1) carotenes, such as lycopene and β-carotene, which are either linear or cyclized hydrocarbons, and (2) xanthophylls, such as zeaxanthin and astaxanthin, which are oxygenated carotene derivatives (1). It is this system of conjugated double bonds, with delocalization of π-electrons spanning the entire molecule, that give carotenoids their distinct light-absorbing and chemical properties. Upon the absorption of light, a π-electron of the conjugated system is excited to a higher energy, unoccupied π^* orbital. This absorption occurs over the range of 400-500 nm, resulting in the characteristic carotenoid shades of yellow, orange, and red (2).

Not only does this conjugated double-bond system contribute to the light-absorbing properties of carotenoids, but it also makes them susceptible to oxidation (3). They readily react with and quench singlet oxygen, potentially allowing them to protect cells from oxidative stress caused by free radicals (2, 4). Because carotenoids are largely hydrophobic, they are often found to be associated with membranes; therefore they can play roles in determining membrane structure, rigidity, and permeability, as well as in affecting signal transduction and cell-to-cell communication by interacting with membrane-associated enzymes (2).

These biochemical properties, in addition to the growing scientific evidence of their health benefits, make carotenoids products of increasing commercial demand (5). In the

nutraceutical and pharmaceutical industries, carotenoids are being marketed for their antioxidant properties and their implicated roles in the treatment and prevention of degenerative diseases and tumorigenesis (6). Carotenoids can now be found in over-the-counter dietary supplements and fortified foods. Due to their bright colors, carotenoids are also used in cosmetics and animal feed, such as in fish food, to improve the physical appearance of organisms (5).

In particular, there are five carotenoids used for these commercial purposes: β-carotene, astaxanthin, canthaxanthin, lycopene, and lutein. β-Carotene is the most widely known carotenoid and has been noted for its role as a vitamin A precursor as well as for its high antioxidant activity; however, there has been a growing interest in the xanthophyll astaxanthin (5). Not only does astaxanthin help maintain the characteristic hue of salmon and is therefore important in aquaculture, but it has also been reported to have a greater antioxidant activity than that of β-carotene (7).

While all of these carotenoids can be found in their natural form, β-carotene, astaxanthin, and canthaxanthin are also made synthetically. Although chemically-synthesized carotenoids currently dominate the market, there is an increasing consumer demand for naturally-derived carotenoids (5). In spite of the abundance of carotenoid-producing organisms, obtaining a high yield of carotenoids by natural production can be more difficult than by synthetic means. The biomass required to generate a profitable amount of carotenoids must be taken into account. Additionally, many organisms that naturally synthesize these compounds possess cell walls, such as plants and some algae, which adds a layer of complexity to the process of extraction from the organism. Indeed, a major obstacle in the bioproduction of carotenoids is extraction, which varies from organism to organism and contributes to high production costs (8).

Halophilic, or salt-loving, archaea such as *Haloferax volcanii*, *Halobacterium salinarum*, and *Haloarcula marismortui*, endogenously produce some carotenoids. These extremophiles can grow aerobically, anaerobically, and/or phototrophically. These organisms also possess the ability to adapt to changes in pH, temperature, and metal-ion concentration, and are resistant to desiccation, exposure to sunlight, and ionizing radiation. For these reasons, halophilic archaea are easily cultivated and studied in laboratory settings (9). *H. volcanii* and *H. salinarum* are the two dominant species of halophilic archaea that act as model organisms because they both have well-defined genomes that are able to be genetically manipulated. *H. volcanii* is advantageous to perform genetic manipulations on because this organism grows quickly and has a genome that is less susceptible to rearrangements in comparison to the genome of *H. salinarum* (10). With available genomic data and tools for molecular manipulation, these organisms may offer a promising new environment for the bioproduction of carotenoids. Their halophilicity may also contribute to more efficient and effective carotenoid extraction procedures, as these organisms lack cell walls and lyse in the presence of water.

H. volcanii predominantly synthesizes the carotenoids phytoene, lycopene, and bacterioruberin (Fig. 1) (11). As in many carotenoid-producing organisms, carotenoid synthesis begins with the condensation of two GGPP molecules into the C_{40} molecule phytoene, a reaction catalyzed by the phytoene synthase enzyme. Phytoene is then converted to lycopene by phytoene desaturase, an enzyme that is present as multiple paralogs in some organisms and that has possible associations with other enzymes involved in carotenoid biosynthesis. One of these enzymes, lycopene elongase, aids in the conversion of lycopene to bacterioruberin (12). Alternatively, in other halophilic archaeal species, lycopene can also be converted to β-carotene

by the enzyme lycopene cyclase; β-carotene then has the potential to be converted to xanthophylls such as astaxanthin (Fig. 1) (13).

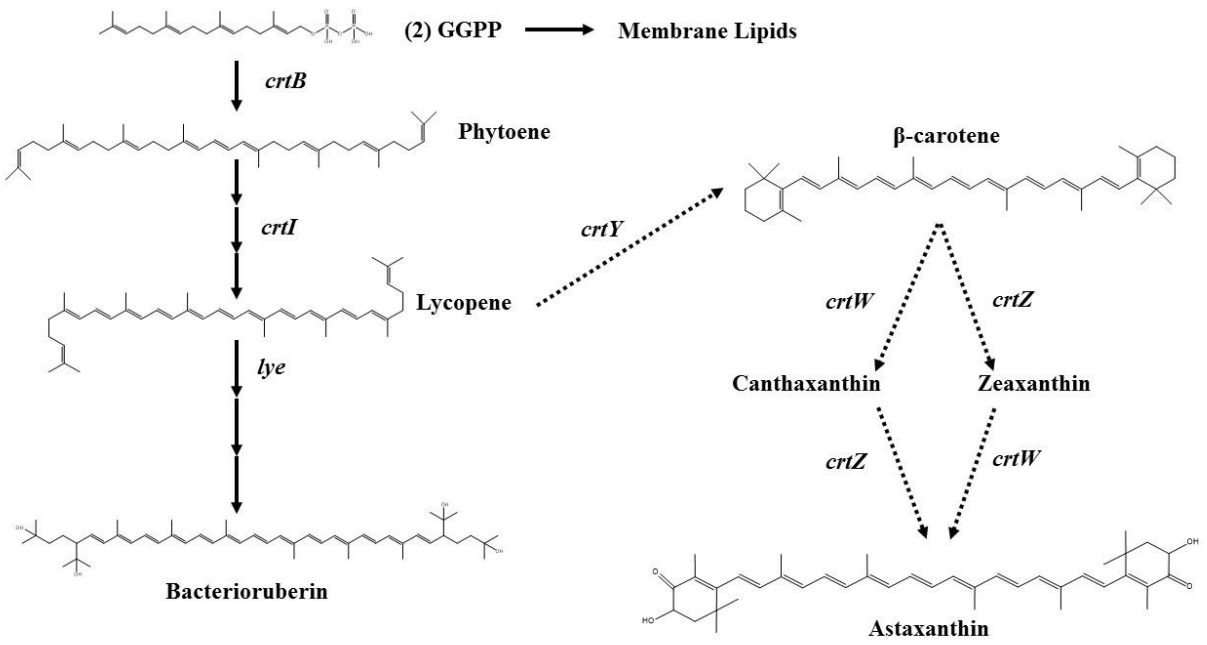

Figure 1. Biosynthetic pathways of bacterioruberin and astaxanthin production. Geranylgeranyl pyrophosphate (GGPP), a molecule that is made of four five-carbon isoprenoid units and that can also be used to make membrane lipids, is converted to phytoene by phytoene synthase (*crtB*). This is then converted to lycopene by phytoene desaturase (*crtI*). Lycopene is a precursor for bacterioruberin, with this reaction catalyzed by lycopene elongase (*lye*). Alternatively, lycopene is converted to β-carotene by lycopene cyclase (*crtY*). β-carotene ketolase (*crtW*) and β-carotene hydroxylase (*crtZ*) work to convert β-carotene to astaxanthin. The carotenoid synthesis pathway endogenous to *Haloferax volcanii* is indicated by solid arrows. Alternative carotenoid synthesis pathways are indicated by dashed arrows.

Bacterioruberin is the carotenoid of highest concentration in *H. volcanii* and amounts to about 82% of total carotenoid compounds, while lycopene contributes only 0.3%. However, *H. volcanii* does not naturally produce large amounts of carotenoids, as these molecules account for a mere 0.04% of the dry weight (11). The yield of carotenoids in *H. volcanii* must be increased for viable production on an industrial scale. Upregulating the first step in this pathway may drive carotenoid production because it biases the pathway towards phytoene synthesis and thus

commits the cells to making carotenoids. Therefore, increasing expression of phytoene synthase through insertion of a highly-active regulatory element should result in a higher carotenoid yield (Fig. 1). In *H. volcanii*, increasing carotenoid production may lead to a build-up of bacterioruberin; however, this carotenoid is not of high demand in comparison with lycopene, β-carotene, and astaxanthin. *H. volcanii* produces only small quantities of lycopene and no β-carotene or astaxanthin. Nevertheless, it synthesizes precursors that have the potential to be converted into these carotenoids in the presence of enzymes from other organisms that promote carotenoid biosynthesis (11). We seek to exploit the innate carotenoid-making abilities of *H. volcanii* to synthesize β-carotene and astaxanthin.

In this work, we show that it is possible to re-engineer the biosynthetic pathway in *H. volcanii* in order to increase carotenoid production and synthesize carotenoids of high demand. The prevention of bacterioruberin synthesis is a necessary step in the re-modeling of this pathway, for it permits an accumulation of lycopene (12). The existence of an *H. volcanii* strain in which the lycopene elongase (*lye*) gene is knocked-out made this step feasible (14). Lycopene production was increased by upregulating expression of phytoene synthase (*crtB*) through the insertion of a modified *ferredoxin* (*fdx*) promoter from *H. salinarum*, which has previously been shown to upregulate transcription in *H. volcanii* (15).

It was necessary to clone the gene for lycopene cyclase (*crtY*) from another halophilic archaeon and express it in *H. volcanii* because *H. volcanii* does not endogenously produce β-carotene (Fig. 1). Both *H. salinarum* and *H. marismortui* have *crtY* in their genomes, but only expression of the *H. marismortui crtY* in *H. volcanii* was found to enable the conversion of lycopene to β-carotene in the presence of *H. marismortui* phytoene desaturase paralogs (*crtI1* and *crtI2*), as well as in the presence of the orthologous *H. volcanii* phytoene desaturase (*crtI*).

Expression of ketolase and hydroxylase enzymes (*crtW* and *crtZ*, respectively) from other halophiles may then allow for the conversion of β-carotene to astaxanthin (Fig. 1). By re-engineering the carotenoid biosynthetic pathway through these genetic manipulations, production and extraction from *Haloferax volcanii* may provide a more effective, efficient, and affordable method of carotenoid synthesis than those currently offered by chemical synthesis or by extraction from plants and algae.

Materials and Methods

Culture conditions

H. volcanii strains were grown in Hv-YPC medium supplemented with 40 µg/mL thymidine (16). Liquid cultures were incubated at 40 °C and 250 rpm. Plates were incubated at 42 °C. *Escherichia coli* DH5α (New England Biolabs, Ipswich, MA) was grown in LB medium supplemented with 100 µg/mL ampicillin at 37 °C. Liquid cultures were grown shaking at 250 rpm.

Strain and plasmid construction

H. volcanii strains were constructed using plasmids and primers found in Tables 1-3. All primers were ordered from Integrated DNA Technologies (Coralville, IA). Synthetic gene 64 was ordered from GenScript (Piscataway, NJ). Plasmids were propagated in *E. coli* DH5α. Gene knockout and replacement mutations were made in *H. volcanii* strain H1209 and its derivatives using a previously described transformation protocol (17, 18). Expression plasmids were constructed from pTA963 and its derivatives (17). Selection and counterselection of *pyrE2* in genomic recombinants were conducted as previously described using plasmids constructed from pTA131 (16). All plasmids introduced into *H. volcanii* were confirmed by sequencing of the added or modified DNA regions (Eurofins Genomics, Louisville, KY). Successful plasmid integration was confirmed by sequencing upstream and downstream regions of the integrated DNA including a primer not found on the integrative plasmid.

In the construction of pRFP270 for inserting RP473 (the modified *fdx* promoter) upstream of *crtB* in the genome of *H. volcanii*, *H. volcanii* DS70 genomic DNA was used as template with primer pairs RP401, RP471 and RP470, RP472 (19). These PCR products were

combined with RP473 in another PCR. The 1761 bp product was amplified with primers RP401 and RP472, which was then cut with *Hind*III and *Xba*I and inserted into the *Hind*III/*Xba*I 3.6 kb fragment of pTA131. The final product included the modified *fdx* promoter directly upstream of *crtB* with flanking sequence to insert into *crtB* locus.

To construct pRFP385 for expression of lycopene cyclase (*crtY*), RFP66 genomic DNA was used as template with primers RP564 and RP565. The 727 bp PCR product was digested with *Nde*I and *EcoR*I and ligated into the *Nde*I/*EcoR*I 8.3 kb fragment of pTA963.

pRFP387 and pRFP388 were derived from pRFP385 in order to place the *Haloarcula marismortui crtI1* and *crtI2* genes downstream of *crtY*. In the construction of pRFP387, RFP66 genomic DNA was used as template with primers RP566 and RP567. The 1524 bp PCR product was digested with *EcoR*I and *BamH*I and ligated into the *EcoR*I/*BamH*I 9.0 kb fragment of pRFP385. Alternatively, for pRFP388, a 1488 bp product derived from PCR of RFP66 genomic DNA with primers RP568 and RP 569 was digested with *EcoR*I and *BamH*I and ligated into the *EcoR*I/*BamH*I 9.0 kb fragment of pRFP385.

To construct pRFP390 for the insertion of genes at the *H. volcanii crtI-lye* locus, a 3.6 kb fragment of pTA131 and a 1980 bp fragment of synthetic gene 64 were ligated after digestion with *Kpn*I and *Xba*I. In order to place *H. marismortui crtI1-crtY* at the *H. volcanii crtI-lye* locus, pRFP390 was digested with *Apa*I and *Bam*-HF to produce a 5.5 kb fragment. pRFP387 was digested with *Apa*I and *EcoR*I-HF to produce a 956 bp fragment, as well as with *Bam*-HF and *EcoR*I-HF to produce a 1557 bp fragment. These fragments were ligated to produce pRFP391.

Plasmids pRFP128, pRFP246, pRFP260, pRFP261, pRFP266, and pRFP267 were previously constructed in this laboratory (Graham and Peck, unpublished).

Table 1. Strains and respective genotypes used in this study

Strain	Genotype	Construction or reference
H1209	*ΔpyrE2 ΔhdrB pitA$_{Nph}$ Δmrr*	(17)
RFP58	H1209 Δ*lye*	(14)
RFP66	*Haloarcula marismortui* ATCC strain #43049	
RFP190	H1209 Δ*crtI*	H1209 - pRFP247 genomic recombinant
RFP211	RFP58 *Δlye::lye(H. salinarum crtY)*	RFP58 - pRFP260 genomic recombinant
RFP231	H1209 with *fdx* promoter upregulating *crtB*	H1209 - pRFP270 genomic recombinant
RFP232	RFP58 with *fdx* promoter upregulating *crtB*	RFP58 - pRFP270 genomic recombinant
RFP233	RFP211 with *fdx* promoter upregulating *crtB*	RFP211 - pRFP270 genomic recombinant
RFP234	RFP233 with *fdx* promoter upregulating *crtB* and *P. haeundaensis crtZ*	RFP233 transformed with pRFP261
RFP235	RFP233 with *fdx* promoter upregulating *crtB* and *P. haeundaensis crtW*	RFP233 transformed with pRFP266
RFP236	RFP233 with *fdx* promoter upregulating *crtB* and *P. haeundaensis crtW* and *crtZ*	RFP233 transformed with pRFP267
RFP302	RFP190 with *H. marismortui crtY* and *crtI1* expressed from a plasmid	RFP190 with pRFP387 transformed
RFP303	RFP190 with *H. marismortui crtY* and *crtI2* expressed from a plasmid	RFP190 with pRFP388 transformed
RFP304	RFP190 with *H. marismortui crtY* expressed from a plasmid	RFP232 with pRFP385 transformed
RFP305	RFP232 *ΔcrtI* with *fdx* promoter upregulating *crtB*	RFP232 - pRFP247 genomic recombinant
TM JCM 10717^{T}	*Haloferax alexandrinus* strain isolated from El-Mallahet, Egypt	(20)
RFP373	RFP305 *lye crtI::H. marismortui crtI1 crtY* with *fdx* promoter upregulating *crtB*	RFP305 - pRFP391 genomic recombinant
RFP403	RFP373 with *P. haeundaensis crtZ* expressed from a plasmid	RFP373 with pRFP261 transformed
RFP404	RFP373 with *P. haeundaensis crtW* expressed from a plasmid	RFP373 with pRFP266 transformed
RFP405	RFP373 with *P. haeundaensis crtZ* and *crtW* expressed from a plasmid	RFP373 with pRFP267 transformed

Table 2. Plasmids used in this study

Plasmid	Relevant Characteristics	Reference
pTA131	Integrative plasmid to allow for gene deletion and replacement in *H. volcanii*	(16)
pTA963	*H. volcanii* expression vector	(17)
pRFP128	Integrative plasmid to insert genes into the *H. volcanii lye* locus	(14)
pRFP247	pTA131- integrative plasmid for *H. volcanii crtI* deletion	This study
pRFP260	pRFP128 with *H. salinarum crtY*	This study
pRFP261	pTA963 with *P. haeundaensis crtZ*	This study
pRFP266	pTA963 with *P. haeundaensis crtW*	This study
pRFP267	pTA963 with *P. haeundaensis crtZ* and *crtW*	This study
pRFP270	pTA131- integrative plasmid to insert *fdx*upstream of *crtB* in *H. volcanii*	This study
pRFP385	pTA963 with *H. marismortui crtY*	This study
pRFP387	pTA963 with *H. marismortui crtY* and *crtI1*	This study
pRFP388	pTA963 with *H. marismortui crtY* and *crtI2*	This study
pRFP390	pTA131- integrative plasmid to insert genes at the *H. volcanii crtI-lye* locus	This study
pRFP391	pRFP390 with *H. marismortui crtY* and *crtI1*	This study

Table 3. Primers and DNA sequences used for plasmid construction

Primers	**Sequence** (Capital letters indicate nt absent in template)	**Description**
Synthetic Gene 64	GGTACCCGCCTCGACGCTCGCGGCGTACGCGGAGAG CGCGACGAGTGCCGCGACGCTCCCCGCGCCGATGGC CGTCGCCGTCGAACGGTTCATATTGTGAACGAACCG ATTGGGATTAATAAGGGGCGCGGTTCCGGCGGAACG GGTGGGTCGACACGGCGGGAGGCCTCAGCGCGTCGC CCGTTTCCACGCCTTGAGGTCCGCGATGTCGCCGTCG AACTCGGCGGGGTCGGCGTCGGTCGCCGCCCAGACG AACAGATCGGCCACGTCGTCGGGGTCGCGGCCCTGC CCGCCGGTGAGGTCGGTGGCGACGAGGCCGGGGTC GACGACCGTCACGGTCCGGTCGCAGTCGGCGGCGAA CTGCCGGACGAGCGCCTCGGCGGCCGCCTTGGAGAC GGCGTACGCGCCCATCCCCGGTTTCGCCTCGCGGGC GATGGAGCCGGAGGGGACGAGGATGCGCCCGTCGT CGGCCATGTGCGGCAGCGCCTCTTTGACCGCCGCGA AGACGCCGCGGACGTTGGTTCTGAGGGTGTCGTCGA ACGCCGCGTACGAGTCCTCGGGCGCGGGCATCTCGC CGGGCGTCCCGTGGGCGACGGCGGCGTTGGCGACGA GTACGTCGATGCGTCCGCCGGCGCGGGCCGCCGTCT CCATCAGGCGCTCCATGTCGAGTTCGTCGCGCACGT CGGCGCGGACTGCGCTGGCGCTGCCGCCGTCGCGTT CGATATCGTTGACGACCGACTGGAGGGCGTCGCCGT CGCGGGCGCAGGCGACGACCGTCGCGCCGGCGCGA CCGAGGGCGCGCGCGACCGCCGCGCCGATTCCGGAA CTCGCACCCGTGACCACCGCGGTGGTGTCGTTCATG CGGGGCCGTAAGGAGGGACCGAGCCTAAAGCTACC CCCCGACGGCGGTCGATTCGGTCAGTCGATTTATGTT CTCTACGTCCTTACGAACGGACGGGCCCACAAGCTT GATATCGAATTCCTGCAGCCCGGGGGATCCACTAGT TCCAGAGCGGCCGCACCTCTGGACCATCGCATTTTTC GGCGCGGCGCCGGGAAGCGCTCGCGCTCGTGCTCGT GCTCGTGCTCGTCTGGCGCGACTCCTGTGCTGTCCCC CAGTCCGACTCGACGCCGCGACGCCGGCCACGGTAG ACGGCCCCGAGTCGTTTCCACTTGAGCAGGCCGAAG CCGAGCAGGATGAGCCCGAAGCCGAGAAGCGTGGT CGGGGTCACGGGCTCCGTGAACAGGAGCCAACTGTA CACCGTCCCGAAGCCGGCGACGGCGTAGGTGACGA GGTTGAGTTCGACCGAGCCGAGACGGGGGAGAAGC GAGAAGTACAGCAGGTAACTGACCGCGCTCGCGAA GACGCCGAGGTAGACGAGGCCGGCGATGCCAGCCA GCGACACGTCGACCTGCGCCAGCGACTCCGTCGGAC TCGCGGCGCTGGCGAGGTGGGTCGCGGCGGCCCCGA CGACCATCGCCCACGCGGTCTGGGCGGCAAACGGCA GGTCGGTCTCGATTCGCTGGGTGAGCACGCCGCCGA GCGCGAACGCCGCCGCGGCGAGCACCAGTATCGCCT	For deletion of the *H. volcanii crtI* and *lye* in order to insert *H. marismortui crtY* and *crtI1*at this locus

	GTCCCGTCGCGTTCGCTCCGAGGAGGTTCGCCGGCT CCGGGTCGGTGACGACGACGAGTCCGAGGAAGCCG ACGGCGACGCCGAGCAGTTCGACCGGGCCGAACCG CTCGTCGGGAAGCCACAGCTTCGCGAAGCCGACGGT CAGTATCGGAACCAACCCCGCGAGCACCGACGCGAC CGCGCTCGGGACGCTCTGCTGACCGATGTTTTGGAG GGCGCTATACCCCGCGAGCGACAGGACCCCGGCCGC GGCGACGACCGCCCAATCGCGTCTCGTCCGGGGTCG CCAGTAGTCGGCGCGCCACGCCGCGTACGGCAACAG AAGCGCCGCGCCGATGTCGAGTCGGAGCGCGGCGTA CAGAACCGGCGGGAACGACTCCAACCCGAGCGTCA CCGCTCTAGACT	
RP184	AAAA<u>CATA***TGA***</u>tggcgtgtccgactcgaca	For insertion of *H. salinarum crtY* into pRFP128; *Nde*I site underlined; stop codon bolded
RP401	AAAA<u>TCTAGA</u>aatcccgttgtcagagaccc	For insertion of *fdx* promoter upstream of *crtB* into pTA131; *Xba*I site underlined
RP411	AAAA<u>TCTAGA</u>ccttgaggtccgcgatgt	For deletion of *H. volcanii crtI* using pTA131; *Xba*I site underlined
RP412	AAA<u>AAAGCTT</u>gcggcgcagtaccagtag	For deletion of *H. volcanii crtI* using pTA131; *Hind*III site underlined
RP413	<u>CTGCTCGATCTCGATCTC</u>agccgagacagaattcatgtc	For deletion of *H. volcanii crtI* using pTA131; underline encodes for EIEIQ sequence that will be inserted in place of *crtI*

RP414	GAGATCGAGATCGAGCAGtgtctcatcagcggtcaact	For deletion of *H. volcanii crtI* using pTA131; underline encodes for EIEIQ sequence that will be inserted in place of *crtI*
RP435	AAAAAGATCT*tca*acgccaccgggcta	For insertion of *H. salinarum crtY* into pRFP128; *Bgl*II site underlined
RP436	AAAACAT*atg*tcggcgcacgcg	For insertion of *P. haeundaensis crtW* into pTA963; *Nde*I site underlined
RP437	AAAAGAATTCGGACTTGCCGTTatgccgtatcacccttggtc	For insertion of *P. haeundaensis crtW* into pTA963; *EcoR*I site underlined
RP438	AAAAGAATTCAAGAAGGAGATATAGATatgtcggcgcacg cg	For insertion of *P. haeundaensis crtW* and *crtZ* into pTA963; *EcoR*I site underlined
RP439	AAAAGGATCCtcatgccgtatcacccttggt	For insertion of *P. haeundaensis crtW* and *crtZ* into pTA963; *BamH*I site underlined
RP440	AAAACATatgacgaacttcctcatcgtcg	For insertion of *P. haeundaensis crtZ* into pTA963; *Nde*I site underlined

RP441	AAAAGAATTCGGACTTGCCGTTacgtccgttcctgcgc	For insertion of *P. haeundaensis crtZ* into pTA963; *Eco*RI site underlined
RP442	AAAAGAATTCAAGAAGGAGATATAGATatgacgaacttcctcatcgtcg	For insertion of *P. haeundaensis crtW* and *crtZ* into pTA963; *Eco*RI site underlined
RP443	AAAAGGATCCtcacgtccgttcctgcg	For insertion of *P. haeundaensis crtW* and *crtZ* into pTA963; *BamH*I site underlined
RP470	GAAGCCGAACTCTGCAGTG*atg*ctcaacgaatcacaggtc	For insertion of *fdx* promoter upstream of crtB into pTA131; overlaps with RP473 3' end; start codon italicized
RP471	CAACGAGGGGTTTTATCCACGcgtttcgtgtgcgtggg	For insertion of *fdx* promoter upstream of crtB into pTA131; overlaps with RP473 5' end
RP472	AAAAAAGCTTgtcgtgagggtgtcgtagtc	For insertion of *fdx* promoter upstream of crtB into pTA131; *Hind*III site underlined
RP473 (*fdx)*	cgtggataaaacccctcgttgacgccgcgggcagcgtcgtgatggcggtcacacccggctttcgtggcagtacgctggcccgaacagcaaagtatttaactggcgaagccgaactctgcagtg	*H. salinarum* modified *fdx* promoter (15)

RP564	AAAACATatgctgtctaccctcacgtatct	For amplification of *H. marismortui crtY*
RP565	AAAAGAATTctcactcccatctgtccatgag	For amplification of *H. marismortui crtY*
RP566	AAAAGAATTCAAGAAGGAGATATAGATatgcgtgatggcctccc	For insertion of *H. marismortui crtI1* downstream of *H. marismortui crtY* in pTA963; *EcoR*I site underlined
RP567	AAAAGGATCCgcagcgtcagtccgcc	For insertion of *H. marismortui crtI1* downstream of *H. marismortui crtY* in pTA963; *BamH*I site underlined
RP568	AAAAGAATTCAAGAAGGAGATATAGATatgagtgacttgtccggtgaag	For insertion of *H. marismortui crtI2* downstream of *H. marismortui crtY* in pTA963; *EcoR*I site underlined
RP569	AAAAGGATCCactcaggcgatatcctcgatga	For insertion of *H. marismortui crtI2* downstream of *H. marismortui crtY* in pTA963; *BamH*I site underlined

RP603	**AAAA<u>CATATG</u>TTGGAGTTATTGCCAACAGCAGTG GAGGGGGTATCG**ctgtggttcctggatgccg	For addition of the *H. salinarum* bacterioopsin (BO) signal sequence to *P. haeundaensis crtW*; for amplification from pRFP266 and insertion into pTA963; *Nde*I cut site underlined; BO sequence bolded
RP604	**AAAA<u>CATATG</u>TTGGAGTTATTGCCAACAGCAGTG GAGGGGGTATCG**acgaacttcctcatcgtcgtg	For addition of the *H. salinarum* BO signal sequence to *P. haeundaensis crtZ*; for amplification from pRFP261 and insertion into pTA963; *Nde*I cut site underlined; BO sequence bolded
RP605	AAAA<u>GAATTC</u>AAGAAGGAGATATAGAT*atg*ttggagttattg ccaacag	For amplification of *P. haeundaensis crtZ* from pRFP394; for insertion into pRFP395; *Eco*RI site underlined

Carotenoid extraction

Carotenoid extraction was performed similarly to methods previously described (12). Taken from *H. volcanii* culture that was grown for about 2 days, 4 mL was added to 96 mL Hv-YPC and 1 mL thymidine (40 µg/mL) and was grown for an additional 16 to 24 hours at 40 °C and 250 rpm. Cultures were centrifuged at 11,000 x g for 15 min at 2 °C and the supernatant was removed. Pellets were washed with 100 mL medium salt solution and centrifuged for an additional 15 min. The supernatant was removed and pellets were centrifuged for an additional 5 min to ensure complete removal of supernatant. Pellets were resuspended in 1 mL media salts, centrifuged for 5 min at 16,000 x g, and the remaining supernatant was removed.

For extraction, pellets were lysed in 1 mL lysis solution (0.032 mg/ml DNase [Sigma-Aldrich]; 0.05% NaN_3) and rotated in the dark until homogenized at 37 °C. Under conditions of low lights to prevent degradation, lysate was added to 13 mL acetone and stirred for 20 min at 7,500 rpm. To the mixture, 7 mL hexane and 1.5 mL water were added and stirred for an additional 2 min. Solutions rested for 5 minutes to allow phases to resolve, and the upper layer was removed and dried under an N_2 stream. Samples were extracted to clearness. For reverse-phase high-performance liquid chromatography and mass spectrometry (RPHPLC-MS), pigments were resuspended in approximately 300 µL hexane, dried again, and re-dissolved in approximately 100 µL ethyl acetate for immediate sampling. For lycopene quantification by UV-vis spectroscopy, samples were resuspended in 3 mL hexane and diluted as necessary. Otherwise, samples were stored at -80 °C.

Reverse phase high-performance liquid chromatography

Samples were fractionated on an Agilent 6230 TOF LC/MS HPLC system using an atmospheric-pressure chemical ionization (APCI) source and a YMC C_{30} column with methanol and ethyl acetate solvents at a flow rate of 1 mL/min. Absorbance was monitored with a photodiode array detector, and molecular weight was analyzed with a time-of-flight mass spectrometer. The solvents used were methanol and ethyl acetate. The solvent change over a 25-min run is described in Table 4.

Table 4. Solvent change during RPHPLC-MS analysis

Time (min)	% ethyl acetate
0	0
2	10
9	30
16	100
18	100
23	10
25	10

A standard curve was generated through analysis of a mixture containing approximately equimolar amounts of commercial lycopene (Sigma-Aldrich), β-carotene (Cayman Chemicals), canthaxanthin (Sigma-Aldrich), zeaxanthin (Cayman Chemicals), and astaxanthin (Sigma-Aldrich). The order of elution was as follows: astaxanthin (4.5 min), zeaxanthin (5.9 min), canthaxanthin (7 min), β-carotene (12.4 min), and lycopene (17.5 min) (Fig. 3A). Carotenoids extracted from biological samples were identified by time of elution in addition to UV-vis and mass spectra (21).

Lycopene and phytoene quantification

Strains RFP58 and RFP232 were grown for 24 hr shaking at 40 °C and 250 rpm. Equal cell amounts from each culture were centrifuged for 5 min at 13 rpm, resuspended in 1 mL Hv-

YPC, and grown at 40 °C and 250 rpm in 9 mL Hv-YPC with 100 µL thymidine (40 µg/mL). After twenty-four hours, two replicates were started from equal cell amounts derived from these cultures, which were centrifuged in the same way, resuspended in 1 mL Hv-YPC, and grown for 24 hr at 40 °C and 250 rpm in 99 mL Hv-YPC 1 mL thymidine (40 µg/mL). Replicates of greatest concentration were centrifuged for extraction as described earlier. Remaining cultures were permitted to grow another 24 hr before centrifugation and extraction.

Samples were analyzed using an Agilent Cary60 UV-vis spectrophotometer. Lycopene and phytoene were identified by their respective λ_{max} values in hexane (lycopene, 472 nm; phytoene, 286 nm), and concentrations were calculated using an average extinction coefficient of 854 L mol^{-1} cm^{-1} for a 1% solution of phytoene and 185,221 L mol^{-1} cm^{-1} for pure lycopene (22).

Comparison of growth rates

RFP58, RFP232, and RFP373 were grown for 24 hr shaking at 40 °C and 250 rpm. Cultures were diluted to an absorbance of 0.005 and grown for another 24 hr under the same conditions. Cultures were diluted to an absorbance of 0.001 and grown for 12 hr shaking at 40 °C and 250 rpm. Absorbance at 660 nm was recorded every 12 hrs until each culture reached stationary phase and absorbance readings stabilized.

Results

Insertion of modified *fdx* promoter leads to increased lycopene and phytoene production

In order to increase overall lycopene production for eventual conversion into β-carotene, upregulation of the first step in the *H. volcanii* biosynthetic pathway is necessary to favor carotenoid synthesis (Fig. 1). A modified *ferredoxin* (*fdx*) promoter, which has been previously indicated in upregulating transcription in *H. volcanii*, was inserted upstream of the *crtB* locus in RFP58 (*H. volcanii* Δ*lye*) by homologous recombination to generate RFP232 (15). This highly-active promoter was expected to increase the presence of phytoene synthase, leading to greater conversion of GGPP to phytoene, which would thereby facilitate lycopene accumulation (Fig. 1).

Colonies of RFP232 were darker red-orange in color compared to the pale red seen for RFP58, suggesting an increase in lycopene production (Fig. 2). Phytoene and lycopene build-up were quantitatively assessed using UV-vis spectroscopy. Carotenoids were extracted from 24 and 48-hr cultures of RFP58 and RFP232. The absorbances for the extracts were measured at 286 nm and 472 nm, the λ_{max} values for phytoene and lycopene, respectively, in order to determine concentrations on a μmol carotenoid per L culture basis in a manner similar to previous studies (22). There was an approximate 46-fold increase in the concentration of phytoene and a 22-fold increase in the concentration of lycopene in 24-hr cultures of RFP232 relative to 24-hr cultures of RFP58, while 48-hr cultures of RFP232 revealed an 86-fold increase in the concentration of phytoene and a 5-fold increase in the concentration of lycopene relative to 48-hr cultures of RFP58 (Fig. 3). Thus, insertion of the modified *fdx* promoter permitted a significant increase in phytoene and lycopene production after both 24 and 48 hr.

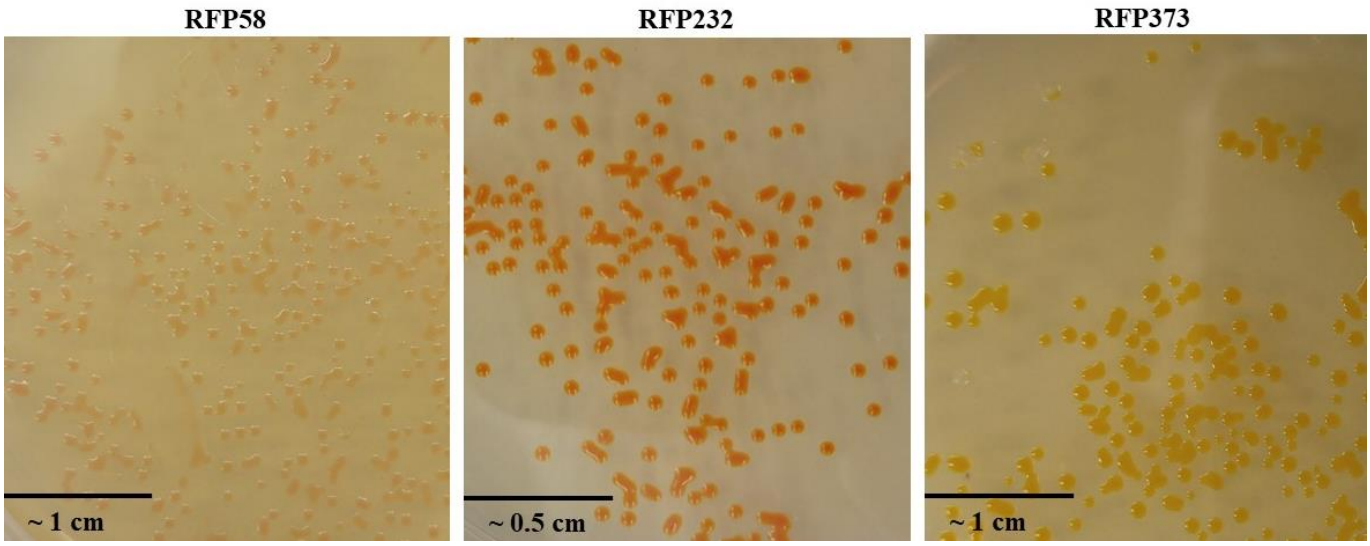

Figure 2. Colony colors of RFP58, RFP232, and RFP373 indicate differing carotenoid production. *Haloferax volcanii* strains RFP58, RFP232, and RFP373 were grown at 40 °C and 250 rpm in liquid Hv-YPC medium supplemented with 40 µg/mL thymidine for 24 to 48 hr. Cultures were diluted and plated on solid media of the same composition. RFP58 (left) synthesizes lycopene. RFP232 (middle) synthesizes an increased amount of lycopene. RFP373 (right) synthesizes β-carotene.

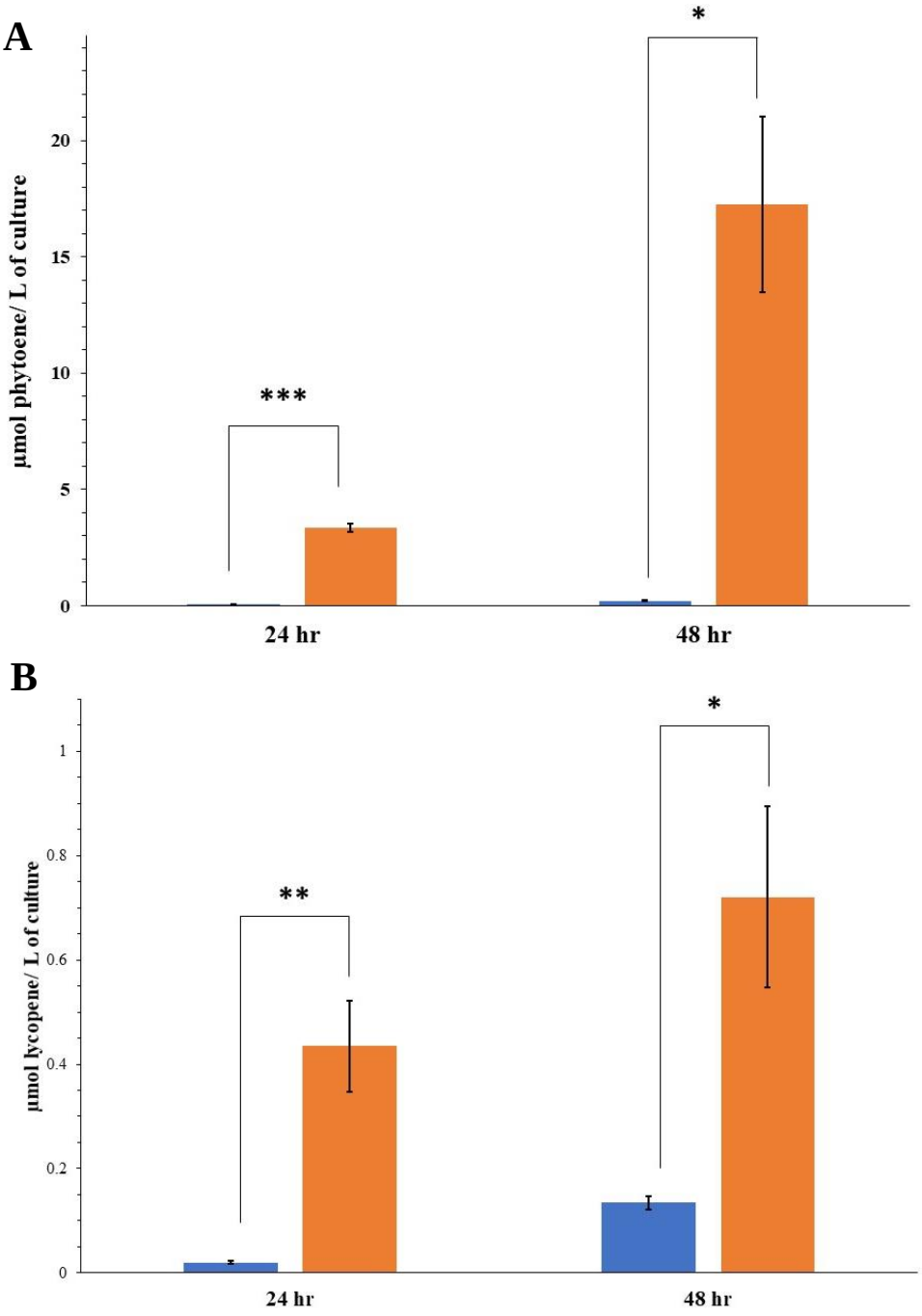

Figure 3. Insertion of *fdx* promoter significantly increases phytoene and lycopene production. Carotenoids were extracted from cultures of RFP58 (blue) and RFP232 (orange) grown for 24 and 48 hrs. A UV-vis spectrophotometer was used to take absorbance readings at 286 nm and 472 nm for respective phytoene (A) and lycopene (B) quantification. Concentrations were calculated on a µmol carotenoid per L culture basis. n= 4 for all but RFP58 24-hr samples, where n= 3. Error bars are ± 1 standard error. A student's T-Test was used to evaluate statistical significance, as indicated by the asterisks. ***= p-value < 0.00001; **= p-value < 0.01; *= p-value < 0.05

Haloarcula marismortui crtY results in β-carotene production

Haloferax volcanii does not endogenously synthesize β-carotene; however, the lycopene reserve in RFP232 can be used to produce β-carotene in the presence of the lycopene cyclase enzyme (*crtY*) that catalyzes this reaction (Fig. 1). Both the halophilic archaea *Halobacterium salinarum* and *Haloarcula marismortui* have *crtY* in their genomes and therefore synthesize β-carotene. Insertion of the *H. salinarum crtY* at the *lye* locus in RFP58 did not result in an observable change in colony color compared to RFP232, which only makes lycopene. Alternatively, the expression of *H. marismortui crtY* from a plasmid resulted in yellow-gold colonies that contrasted the red-orange colonies of RFP232, its parental strain (data not shown).

In order to determine if RFP233 and RFP304 were producing β-carotene, reverse phase high-performance liquid chromatography (RP-HPLC), mass spectrometry, and UV-vis spectroscopy were used for separation and subsequent identification of carotenoids present in extracted cell pellets of these strains. While both strains produced lycopene, only pellets from RFP304 contained measurable amounts of β-carotene (Fig. 4).

Other proteins found in *H. salinarum* have been previously expressed in *H. volcanii* (12, 14). The fact that the *H. salinarum crtY* did not result in β-carotene production is curious. This result may indicate that certain interactions with other enzymes involved in carotenoid biosynthesis are required for *H. salinarum* phytoene synthase to function. Whereas *H. volcanii* has only one copy of *crtI* in its genome and does not make rhodopsins, which are proteins with prosthetic groups that are synthesized from β-carotene, *H. salinarum* has three copies, *H. marismortui* has two copies, and both make rhodopsins (23, 24). The latter two species also produce a variety of carotenoids that includes β-carotene, whereas *H. volcanii* predominantly synthesizes bacterioruberin and to a lesser extent lycopene (11). While the only form of phytoene

synthase may interact with lycopene elongase in *H. volcanii*, the orthologous forms found in *H. salinarum* and *H. marismortui* may interact with additional carotenoid biosynthetic enzymes.

Using Geneious, a phylogenetic tree of enzymes native to *H. salinarum* and *H. marismortui* with homology to the *H. volcanii crtI* was constructed. Of these homologous enzymes, the *H. marismortui crtI1* was predicted to be less closely related to the *crtI* of *H. volcanii* and therefore suggests possible associations with enzymes other than lycopene elongase, such as lycopene cyclase. Therefore, *H. marismortui crtI1* and *crtY* were integrated at the *lye-crtI* locus by homologous recombination in RFP232. This strain, RFP373, had colonies colored similarly to that of RFP304, likely indicating synthesis of β-carotene via expression of these enzymes that are nonendogenous to *H. volcanii* (Fig. 2).

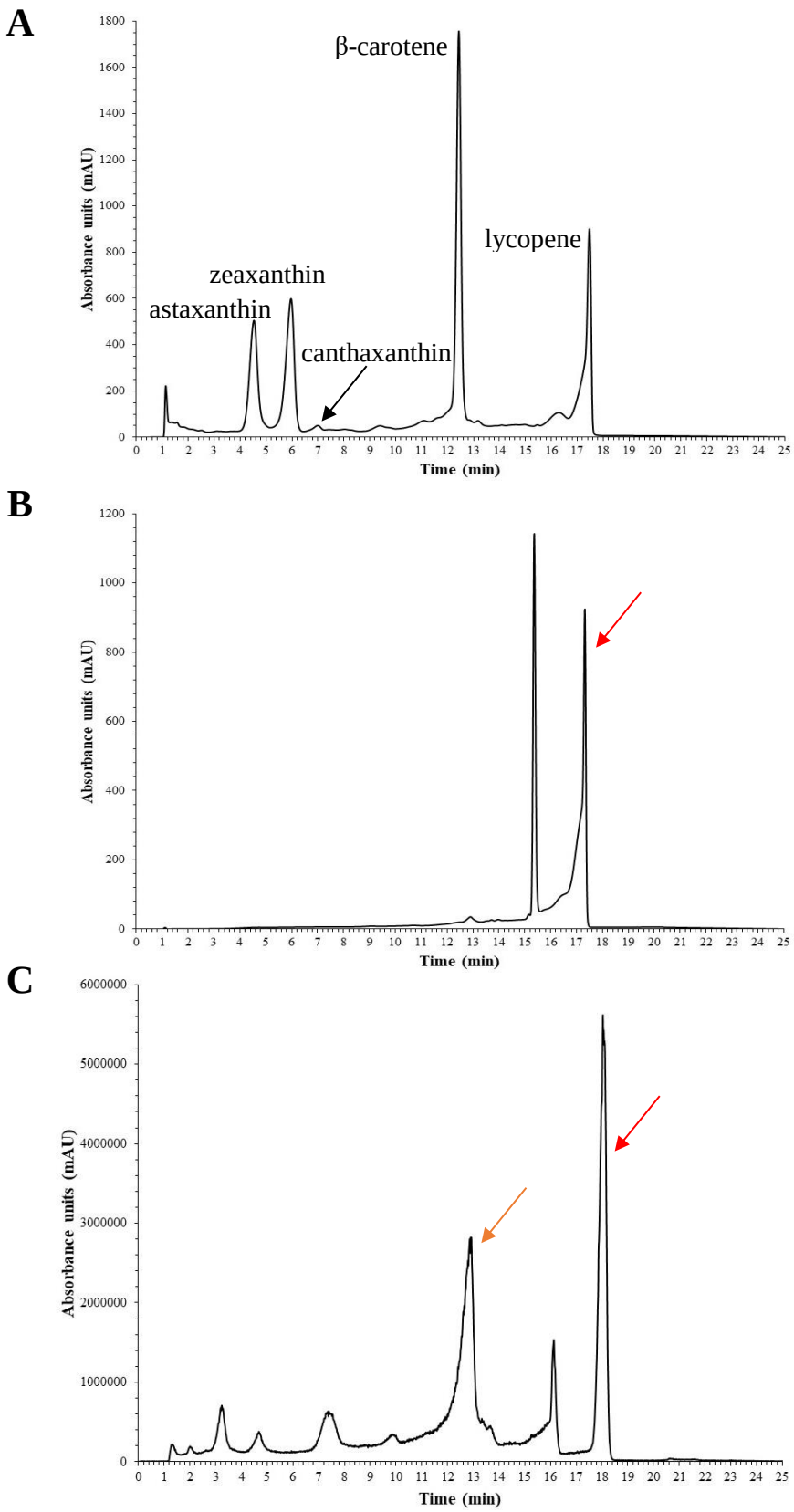

Figure 4. *H. marismortui crtY* yields β-carotene. A standard solution containing relevant carotenoids was separated by HPLC (A). Carotenoids were extracted from cell pellets of RFP233 (B) and RFP304 (C) and separated by HPLC. Elution patterns were compared to the standard (A). Red arrows indicate elution of lycopene and the orange arrow indicates elution of β-carotene. Mass spectra of the peaks indicated by the colored arrows were analyzed in order to confirm the presence of lycopene and β-carotene. (D) Lycopene standard; (E) Lycopene from RFP233; (F) Lycopene from RFP304; (G) β-carotene standard; (H) β-carotene from RFP304

D

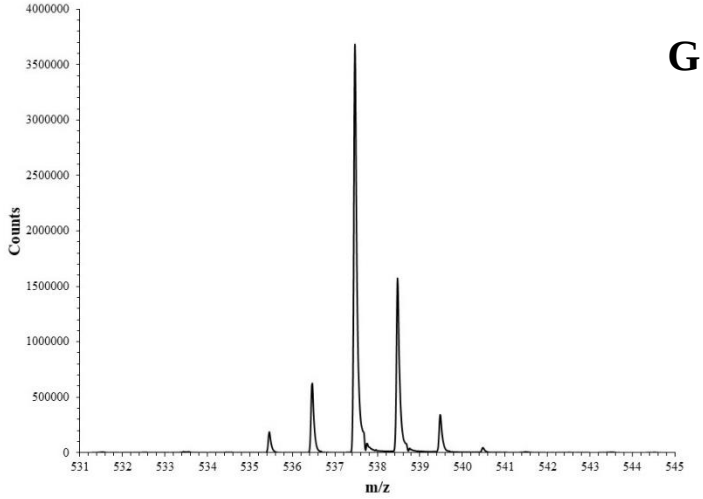

G

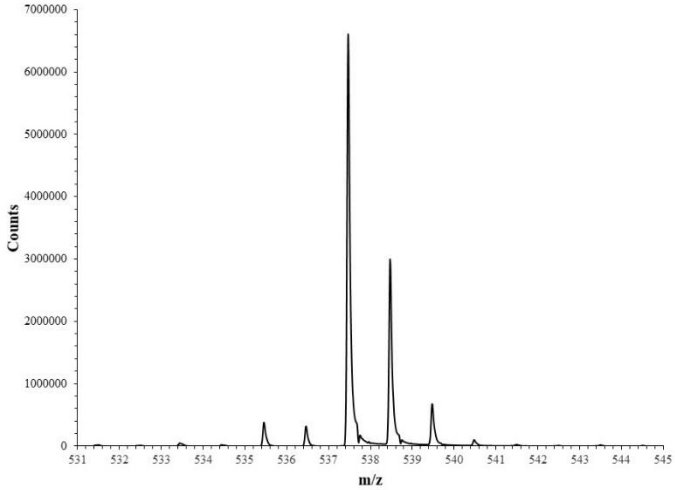

E

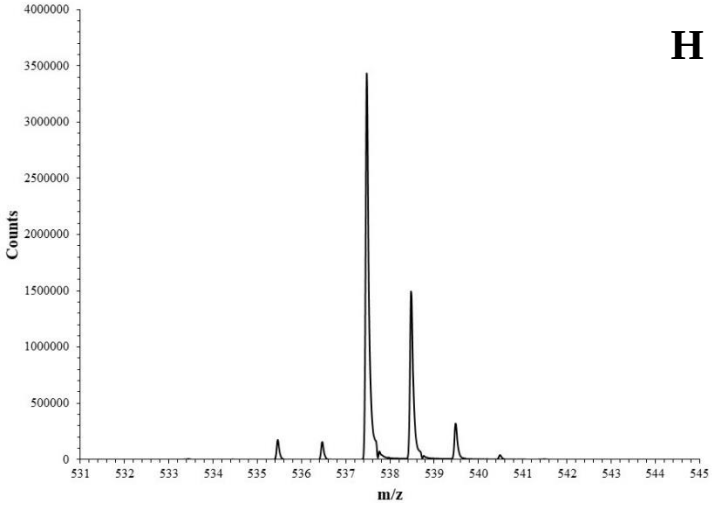

H

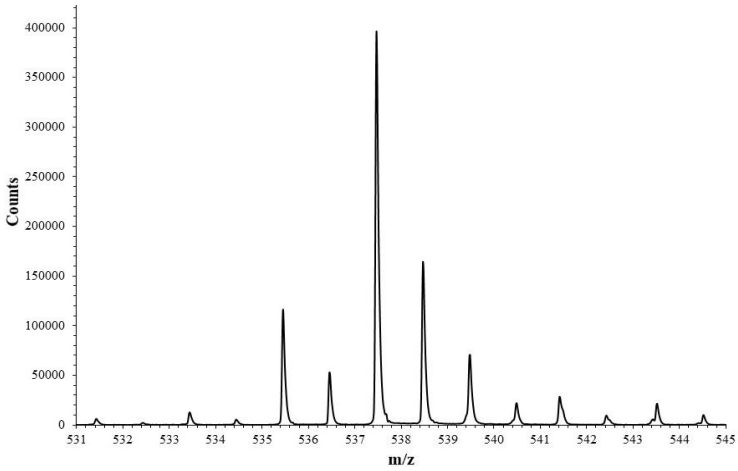

F

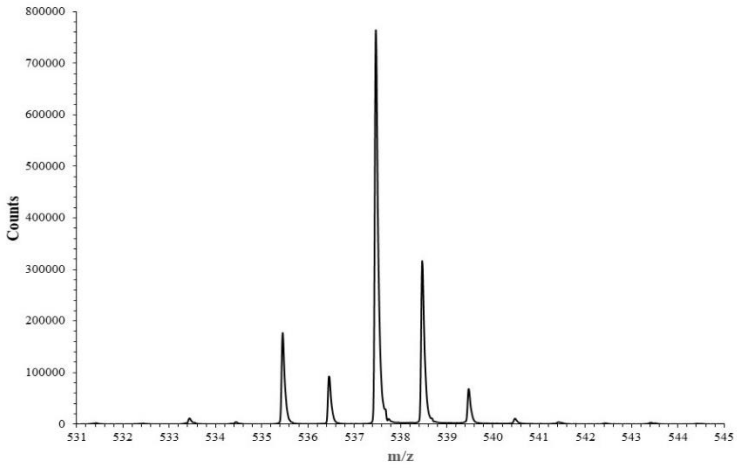

Modified *fdx* promoter increases length of lag phase

Observations of culture growth indicated that cultures of RFP232 were reaching saturation more slowly than cultures of RFP58, its parental strain, and the colonies of RFP232 were smaller than those of RFP58 (Fig. 2). Interestingly, cultures and colonies of RFP373 did not appear to share this phenotype of slowed or impaired growth. Both RFP232 and RFP373 have the modified *fdx* promoter inserted upstream of *crtB* with the intention of upregulating carotenoid synthesis. However, by biasing metabolism to produce carotenoids, there may be less GGPP available for the production of membrane lipids, thus potentially slowing growth (Fig. 1). In order to evaluate the impact of the modified *fdx* promoter on growth, cultures of RFP58, RFP232, and RFP373 were monitored by absorbance (Fig. 5). In comparison to RFP58, the lag phase of growth for RFP232 was extended by about 18 hrs, while that of RFP373 was extended by about 12 hrs. After 84 hrs, however, both RFP232 and RFP373 achieved higher absorbance values than RFP58. These data suggest that, while the lag phase of growth was lengthened, long term archaeal growth was not severely impacted.

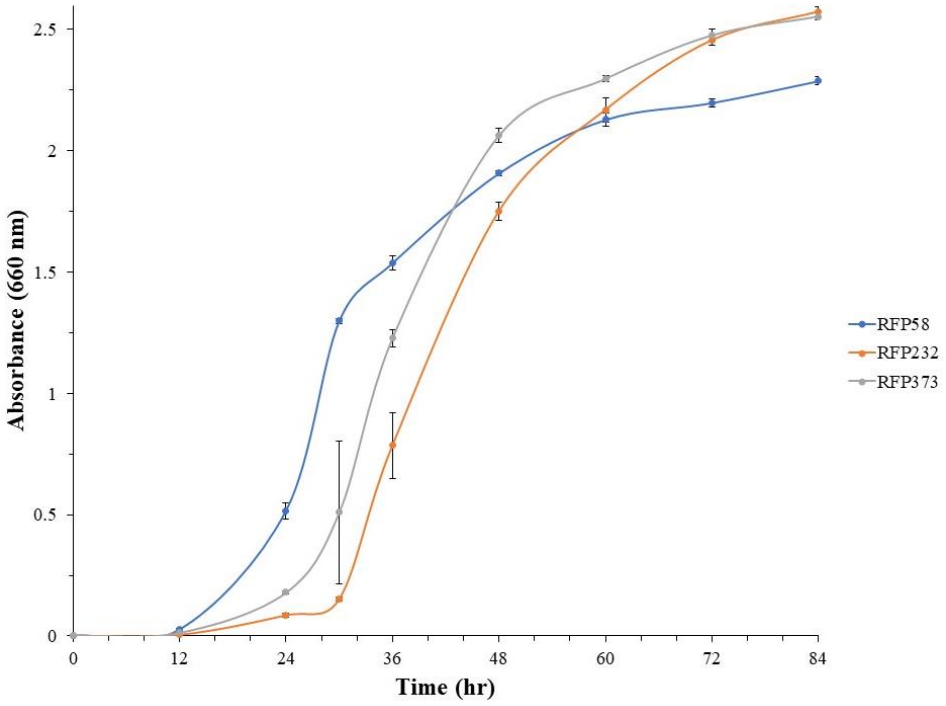

Figure 5. Insertion of modified *fdx* promoter increases lag phase. Cultures of RFP58, RFP232, and RFP373 were grown shaking at 40 °C, and growth was monitored by absorbance at 660 nm. Each point is an average of 3 to 6 cultures. Error bars indicate ±1 standard error.

Paracoccus haeundaensis crtW and *crtZ* do not yield further carotenoid production

Because the colony color of RFP373 suggested the production of β-carotene (Fig. 2), the logical next steps involved expressing other nonendogenous enzymes that would also contribute to carotenoid synthesis. *Paracoccus haeundaensis* is an astaxanthin-producing bacterium that has *crtW* and *crtZ* genes encoding ketolase and hydroxylase enzymes, respectively, which act to convert β-carotene to astaxanthin through canthaxanthin and/or zeaxanthin intermediates (Fig. 1) (25). Therefore, strains RFP403, RFP404, and RFP405 were constructed via transformation of plasmids into RFP373 that would allow for the expression of *crtZ*, *crtW*, or both *crtZ* and *crtW*, respectively. The carotenoids contained in cell pellets of these strains were analyzed using RP-HPLC, mass spectrometry, and UV-vis spectroscopy. Zeaxanthin, canthaxanthin, and astaxanthin were not detected in these strains; however, all three strains showed the presence of β-carotene, confirming that RFP373 synthesizes this carotenoid (Fig. 6).

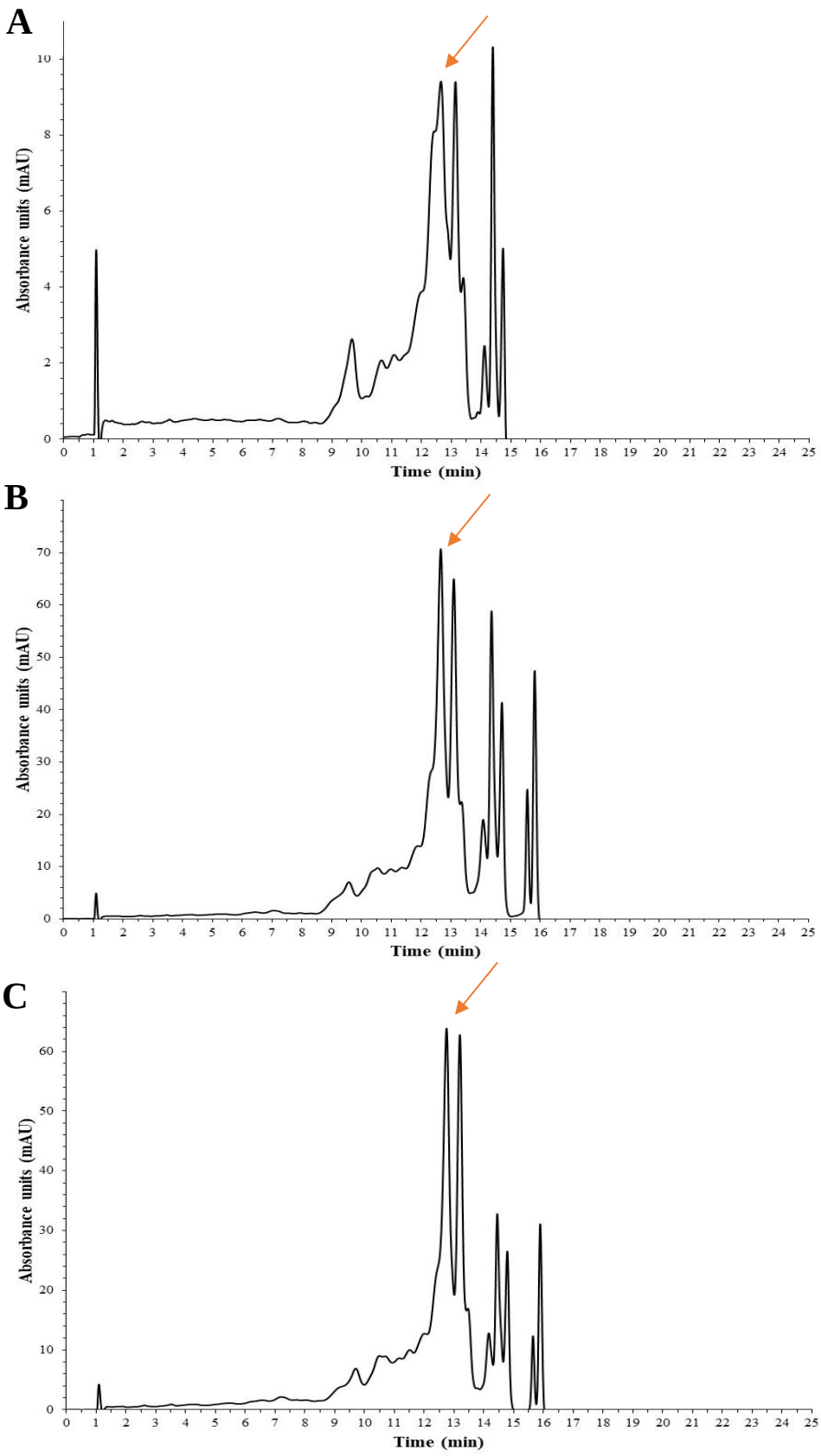

Figure 6. RFP403, 404, and 405 synthesize β-carotene. Carotenoids were extracted from cell pellets of RFP403 (A), RFP404 (B), and RFP405 (C) and separated by HPLC. Elution patterns were compared to the standard (Fig. 4A). Orange arrows indicate β-carotene. Mass spectra of the peaks designated by the orange arrows were analyzed in order to confirm the presence of β-carotene (Fig. 4G) in these strains (D, E, and F, respectively).

D

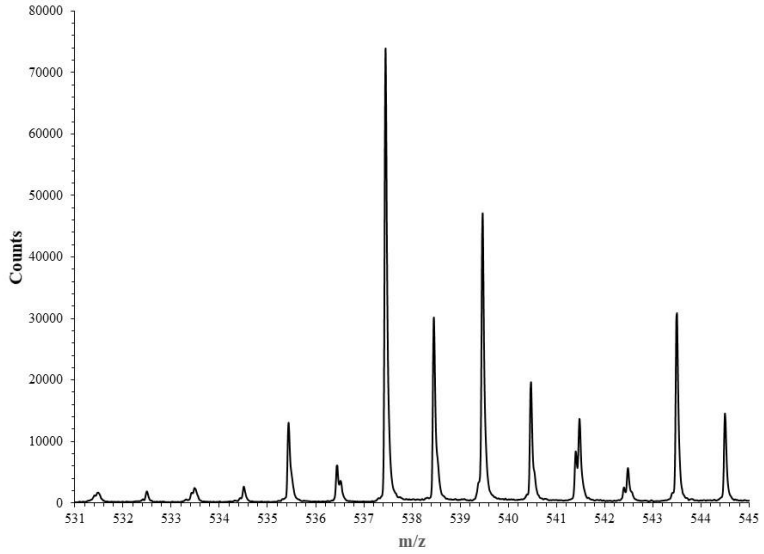

E

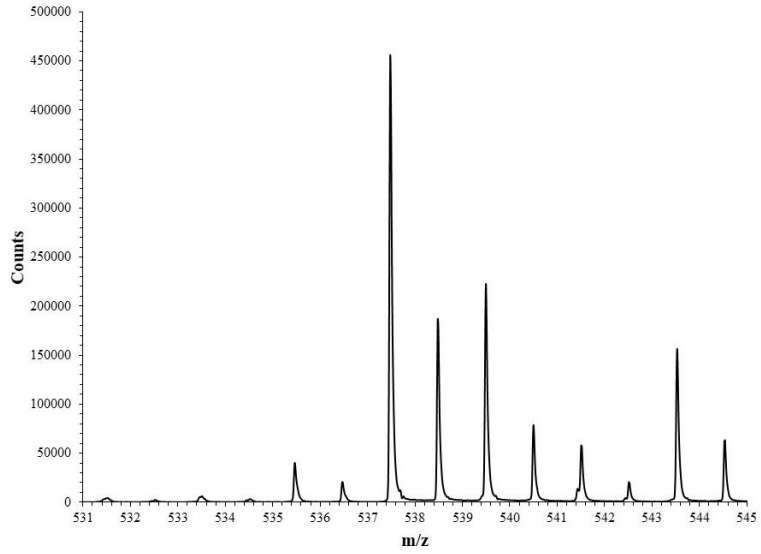

F

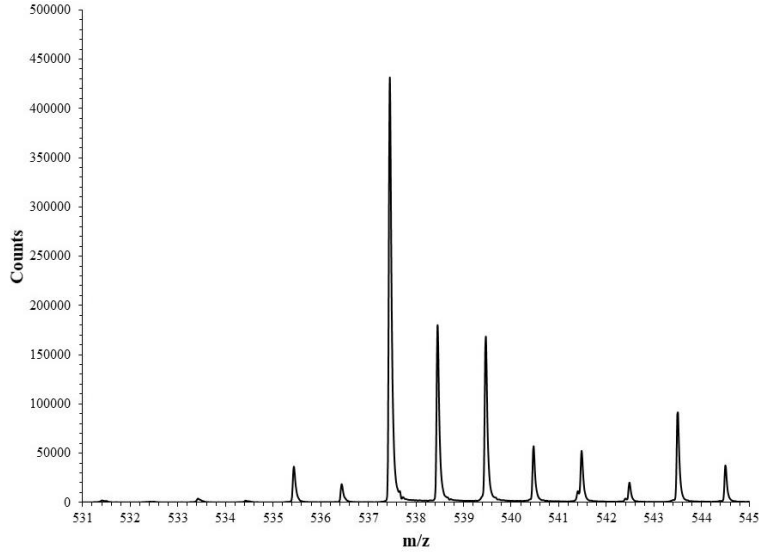

Discussion

We were seeking to capitalize on the innate carotenoid biosynthesis pathway of *Haloferax volcanii* in order to 1) increase overall carotenoid production and 2) to produce carotenoids of high demand, such as lycopene, β-carotene, and astaxanthin (5). In this work, it was found that carotenoid production could be increased by insertion of a highly-active promoter before the *crtB* gene in *H. volcanii*. Cells with the modified *fdx* promoter upstream of *crtB* showed higher levels of phytoene and lycopene production (Fig. 3), which suggests that the promoter acts to increase the transcription of *crtB,* therefore producing more phytoene synthase enzymes for increased synthesis of phytoene and the subsequent conversion of this phytoene into lycopene. The large lycopene reserve available allowed for the production of β-carotene in the presence of the *H. marismortui* lycopene cyclase, thus allowing for the biosynthesis of this highly desired carotenoid, which is a process that does not occur natively in *H. volcanii* cells (Fig. 1).

Because the modified promoter biased the pathway to favor the conversion of GGPP to phytoene instead of membrane lipids, it was possible that having the modified *fdx* promoter upstream of *crtB* was impacting the growth of *H. volcanii*. Although the time spent in the lag phase of growth was extended in the strains possessing the promoter, this slow-growing phenotype was ameliorated after about 56 hrs, and after 84 hrs, these strains reached higher absorbance values than the strain without the modified promoter (Fig. 5). These observations suggest that the modified *fdx* promoter upstream of *crtB* can allow for an enhancement of carotenoid synthesis without greatly impacting the growth rate. These characteristics would be valuable from an industrial standpoint, for it would not take substantially longer to get a significantly greater concentration of carotenoids.

Since β-carotene is a precursor for zeaxanthin, canthaxanthin, and astaxanthin, then *H. volcanii* strains with a hydroxylase (*crtZ*) and/or a ketolase (*crtW*) should be able to synthesize these derivatives (Fig. 1). The inability of *H. volcanii* strains expressing *P. haeundaensis crtZ* and *crtW* to synthesize carotenoids that are derived from β-carotene may indicate that the putative transmembrane proteins encoded by these genes were not efficiently reaching the cell membrane and therefore could not function properly to convert β-carotene into zeaxanthin, canthaxanthin, or astaxanthin. One way to potentially improve the movement of the hydroxylase and ketolase enzymes to the cell membrane includes altering their signal peptide sequences such that they are effectively recognized by *H. volcanii* machinery. Although the transport of proteins to the membrane via this sequence is not well understood in Archaea, it is thought that proteins destined for the membrane or for secretion are synthesized with a signal peptide sequence at the N terminus in order to be recognized by a signal recognition particle (SRP). The SRP interacts with FtsY, a receptor, which allows for the complex to be brought to the membrane. Hydrolysis of GTP is thought to cause the release of the SRP and FtsY from the complex, thereby transferring the ribosome to the SecYEDF translocation machinery and allowing for integration of the growing peptide into the membrane (26).

The *Halobacterium salinarum* transmembrane protein bacterioopsin (BO), which has a known signal peptide sequence, has been successfully expressed in *H. volcanii* and therefore must be effectively transported to the membrane (14). Attachment of this sequence to the N termini of *P. haeundaensis* ketolase and hydroxylase may therefore direct their movement towards the membrane, thus improving their functionality in a nonnative environment and potentially allowing for canthaxanthin, zeaxanthin, and astaxanthin production.

Conclusion

This work has revealed the potential of using *Haloferax volcanii* for the bioproduction of carotenoids on an industrial scale. Not only is *H. volcanii* amenable to extraction procedures, but *H. volcanii* was shown to be able to withstand an upregulation of carotenoid synthesis without compromising efficiency, thus allowing for increased carotenoid production in a cost-effective and time-effective manner. It was also shown to be able to express the gene encoding for *H. marismortui* lycopene cyclase for β-carotene synthesis, a process that does not occur endogenously in wild-type *H. volcanii*. While the *P. haeundaensis* ketolase and hydroxylase enzymes were not shown to be functional in *H. volcanii*, future studies directed at optimizing methods to express these genes may eventually allow *H. volcanii* to also synthesize astaxanthin. These aforementioned characteristics make *Haloferax volcanii* a promising candidate for natural synthesis of commercially-desired carotenoids.

References

1. Sajilata MG, Singhal RS, Kamat MY. 2008. The carotenoid pigment zeaxanthin - A review. Compr Rev Food Sci Food Saf 7:29-49.
2. Britton G. 1995. Structure and properties of carotenoids in relation to function. FASEB J 9:1551-8.
3. Krinsky NI. 1998. The antioxidant and biological properties of the carotenoids. Ann N Y Acad Sci 854:443-7.
4. Bendich A, Olson JA. 1989. Biological actions of carotenoids. FASEB J 3:1927-32.
5. Vílchez C, Forján E, Cuaresma M, Bédmar F, Garbayo I, Vega JM. 2011. Marine Carotenoids: Biological Functions and Commercial Applications. Marine Drugs 9:319-333.
6. Guerin M, Huntley ME, Olaizola M. 2003. *Haematococcus* astaxanthin: applications for human health and nutrition. Trends Biotechnol 21:210-6.
7. Goswami G, Chaudhuri S, Dutta D. 2010. The present perspective of astaxanthin with reference to biosynthesis and pharmacological importance. World J Microbiol Biotechnol 26:1925-1939.
8. Mezzomo N, Ferreira SRS. 2016. Carotenoids functionality, sources, and processing by supercritical technology: A review. Journal of Chemistry 2016.
9. DasSarma S. 2007. Extreme microbes. American Scientist 95:224-231.
10. Leigh JA, Albers SV, Atomi H, Allers T. 2011. Model organisms for genetics in the domain Archaea: methanogens, halophiles, *Thermococcales* and *Sulfolobales.* FEMS Microbiol Rev 35:577-608.

11. Ronnekleiv M. 1995. Bacterial carotenoids 53∗ C50-carotenoids 23; carotenoids of *Haloferax volcanii* versus other halophilic bacteria. Biochem Syst Ecol 23:627-634.

12. Dummer AM, Bonsall JC, Cihla JB, Lawry SM, Johnson GC, Peck RF. 2011. Bacterioopsin-Mediated Regulation of Bacterioruberin Biosynthesis in *Halobacterium salinarum*. J Bacteriol 193:5658-5667.

13. Mann V, Harker M, Pecker I, Hirschberg J. 2000. Metabolic engineering of astaxanthin production in tobacco flowers. Nat Biotechnol 18:888-92.

14. Peck RF, Plesa AM, Graham SM, Angelini DR, Shaw EL. 2017. Opsin-Mediated Inhibition of Bacterioruberin Synthesis in Halophilic Archaea. J Bacteriol 199.

15. Danner S, Soppa J. 1996. Characterization of the distal promoter element of halobacteria in vivo using saturation mutagenesis and selection. Mol Microbiol 19:1265-76.

16. Allers T, Ngo HP, Mevarech M, Lloyd RG. 2004. Development of additional selectable markers for the halophilic archaeon *Haloferax volcanii* based on the *leuB* and *trpA* genes. Appl Environ Microbiol 70:943-53.

17. Allers T, Barak S, Liddell S, Wardell K, Mevarech M. 2010. Improved strains and plasmid vectors for conditional overexpression of His-tagged proteins in *Haloferax volcanii*. Appl Environ Microbiol 76:1759-69.

18. Cline SW, Lam WL, Charlebois RL, Schalkwyk LC, Doolittle WF. 1989. Transformation methods for halophilic archaebacteria. Can J Microbiol 35:148-52.

19. Wendoloski D, Ferrer C, Dyall-Smith ML. 2001. A new simvastatin (mevinolin)-resistance marker from *Haloarcula hispanica* and a new *Haloferax volcanii* strain cured of plasmid pHV2. Microbiology 147:959-64.

20. Asker D, Ohta Y. 2002. Production of canthaxanthin by *Haloferax alexandrinus* under non-aseptic conditions and a simple, rapid method for its extraction. Appl Microbiol Biotechnol 58:743-50.

21. van Breemen RB, Dong L, Pajkovic ND. 2012. Atmospheric Pressure Chemical Ionization Tandem Mass Spectrometry of Carotenoids. Int J Mass Spectrom 312:163-172.

22. Butnariu M. 2016. Methods of Analysis (Extraction, Separation, Identification and Quantification) of Carotenoids from Natural Products. J Ecosys Ecograph 6.

23. Baliga NS, Bonneau R, Facciotti MT, Pan M, Glusman G, Deutsch EW, Shannon P, Chiu Y, Weng RS, Gan RR, Hung P, Date SV, Marcotte E, Hood L, Ng WV. 2004. Genome sequence of *Haloarcula marismortui*: A halophilic archaeon from the Dead Sea. Genome Res 14:2221-2234.

24. Ng WV, Kennedy SP, Mahairas GG, Berquist B, Pan M, Shukla HD, Lasky SR, Baliga NS, Thorsson V, Sbrogna J, Swartzell S, Weir D, Hall J, Dahl TA, Welti R, Goo YA, Leithauser B, Keller K, Cruz R, Danson MJ, Hough DW, Maddocks DG, Jablonski PE, Krebs MP, Angevine CM, Dale H, Isenbarger TA, Peck RF, Pohlschroder M, Spudich JL, Jung K-H, Alam M, Freitas T, Hou S, Daniels CJ, Dennis PP, Omer AD, Ebhardt H, Lowe TM, Liang P, Riley M, Hood L, DasSarma S. 2000. Genome sequence of *Halobacterium* species NRC-1. Proc Natl Acad Sci USA 97:12176-12181.

25. Lee JH, Kim YS, Choi T-J, Lee WJ, Kim YT. 2004. *Paracoccus haeundaensis* sp. nov., a Gram-negative, halophilic, astaxanthin-producing bacterium. Int J Syst Evol Microbiol 54:1699-1702.

26. Zwieb C, Eichler J. 2002. Getting on target: The archaeal signal recognition particle. Archaea 1:27-34.